

# Newly observed $\kappa(2600)$ and the highly excited states of $K_0^*$ family

Cheng-Qun Pang<sup>1,2,3,\*</sup>, Hao Chen<sup>1,†</sup> and Yun-Hai Zhang<sup>4,‡</sup>

<sup>1</sup>College of Physics and Electronic Information Engineering, Qinghai Normal University, Xining 810000, China

<sup>2</sup>Joint Research Center for Physics, Lanzhou University and Qinghai Normal University, Xining 810000, China

<sup>3</sup>Lanzhou Center for Theoretical Physics, Key Laboratory of Theoretical Physics of Gansu Province, Lanzhou University, Lanzhou, Gansu 730000, China,

<sup>4</sup>College of Physics and Electronic Engineering, Heze University, Heze 274015,

(Dated: March 18, 2025)

We conducted a study using the modified Godfrey-Isgur (MGI) quark model and quark pair creation model (QPC model) to investigate the spectrum and two body strong decays of the newly discovered  $\kappa(2600)$  meson in LHCb collaboration. Our analysis revealed that this resonant can be assigned as the fourth radial excitation within the  $0^+$  light strange meson family. Furthermore, we predicted additional radial excitations in this meson family and systematically discussed their spectra, decay behaviors, and branching ratios. These results provide critical guidance for future to identify their signatures in experiments.

PACS numbers:

## I. INTRODUCTION

Recently, the LHCb Collaboration reported the discovery of a new resonance state (or named  $K_0^*(2600)$  in Particle Data Group [1]) in the  $B^- \rightarrow (K_S^0 K^- \pi^+) K^+$  decay channel, with a statistical significance of  $26.6\sigma$ , by analyzing the invariant mass spectrum of  $K\pi$ . The new resonance has the mass and the width of  $2662 \pm 59 \pm 201$  MeV and  $480 \pm 47 \pm 72$  MeV, respectively [2]. This discovery intrigued us to investigate whether the  $\kappa(2600)$  could belong to the  $J^P = 0^+$   $K$  mesons family.

$P$ -wave  $K$  mesons have three  $J$  numbers under the coupling of spin and orbital angular momentum,  $^{2S+1}L_J = ^1P_1$ ,  $^3P_0$ , and  $^3P_2$ . Li et al. discussed a new structure  $X(2085)$  in  $J^P = 1^+$   $K$  meson family, and investigated the other members of this meson family [3]. In our previous work, we studied the  $K_2^*$  meson family, especially the  $K_2^*(1980)$  [4]. For the low-lying excited states of  $0^+$  light strange meson family,  $K_0^*(1430)$  is the ground state, and  $K_0^*(1950)$  can be its first excited state [5, 6]. For the lowest scalar  $\kappa(700)$ , it is widely believed that it may be an exotic state [7–12]. Wang et al. identify that  $K_0^*(2130)$  can be assigned as the second excited state of  $0^+$  light strange meson family [13]. In Ref. [13],  $K_0^*(4P)$  has a mass and width of 2404 MeV and 180 MeV, respectively, whereas its mass was 2424 MeV in our previous work [6]. It is obvious that  $\kappa(2600)$  couldn't be  $K_0^*(4P)$  state. The internal structure of this state, as well as the nature of the highly excited states of the  $0^+$  light strange meson family, becomes an interesting issue.

Regge trajectories are an efficient method for investigating the spectrum of meson families [14, 15]. The relation holds for the masses and radial quantum numbers of mesons within the same meson family

$$M^2 = M_0^2 + (n - 1)\mu^2, \quad (1.1)$$

where  $M_0$  denotes the mass of the ground state,  $n$  represents

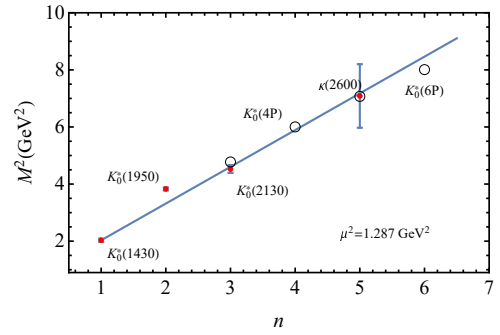


FIG. 1: The Regge trajectories for the  $K_0^*$  family. Here, open circles represent theoretical (MGI model) values, and filled geometries indicate experimental measurements. The radial quantum number, denoted by  $n$ , corresponds to the meson in question.

the radial quantum number of the corresponding meson with the mass  $M$ , and  $\mu^2$  is the trajectory slope. For the  $K_0^*$  family, we adopt  $\mu^2 = 1.287$  GeV<sup>2</sup> as depicted in Fig. 1.

By analyzing the Regge trajectory, the results demonstrate that  $K_0^*(1430)$ ,  $K_0^*(1950)$ , and  $K_0^*(2130)$  are  $1P$  state,  $2P$  state, and  $3P$  state, respectively. The situation for the  $\kappa(2600)$  is less straightforward than expected. The new observed state,  $\kappa(2600)$  can be a good candidate of the fifth radially excited state of  $K_0^*(1430)$ . The  $K_0^*(4P)$  is still misty. The mass of  $K_0^*(4P)$  given by MGI model consists with the value from the Regge trajectory and the mass of  $K_0^*(6P)$  provided by the MGI model is slightly smaller than the one given by the Regge trajectory.

Mass spectra and two body strong decay are two effective analysis methods to study the internal structures of mesons. Via the simple mass analysis, we find that  $\kappa(2600)$  can be arranged as the fifth radially excited state of  $K_0^*(1430)$ . This preliminary conclusion needs to be substantiated with more quantitative analysis. We will study the mass spectra of the  $0^+$  light strange meson family using the MGI model. In 1985, Godfrey and Isgur proposed the Godfrey-Isgur (GI) quark model for describing relativistic meson spectra with great success, exactly

\*Electronic address: xuehua45@163.com

†Electronic address: chen hao\_qhnu@outlook.com

‡Electronic address: wlzyh@163.com

for low-lying mesons [16] and for excited states, the screened potential must be taken into account for coupled-channel effect [17–24]. We also study the two strong decays of the  $0^+$  light strange meson family through QPC model which was initially formulated by Micu [25] and is widely applied to the OZI-allowed two-body strong decays of mesons in Refs. [4, 6, 20–24, 26–46].

The paper is organized as follows: In Sec. II, we briefly reviewed the Regge trajectory, the MGI model, and the  $^3P_0$  model. In Sec. III, the obtained masses of the  $K_0^*$  family are presented and compared with available experimental data and other results from different methods. Then, we systematically study the OZI-allowed two-body strong decay behaviors of the newly observed  $\kappa(2600)$  and predicted states  $K_0^*(4P)$  state and  $K_0^*(6P)$  state. Finally, a conclusion is given in Sec. IV.

## II. MODELS EMPLOYED IN THIS WORK

In this work, we employ two models, the MGI model and the QPC model, which will be introduced in this section.

### A. The modified GI model

1985, Godfrey and Isgur proposed the Godfrey-Isgur (GI) quark model for describing relativistic meson spectra with great success, exactly for low-lying mesons [16]. To describe the excited states well, people introduce the screened potential term [17–24]. Then, Song et al. propose the MGI model [47] based on GI model. And it has great success in calculating light hadron spectroscopy [20–24]. In the MGI model, the Hamiltonian reads

$$\tilde{H} = \sum_i (m_i^2 + \mathbf{p}_i^2)^{1/2} + \tilde{V}^{\text{eff}}, \quad (2.1)$$

where  $m_i$  denotes the mass of the quark and antiquark, and  $\tilde{V}^{\text{eff}}$  includes short-range  $\gamma^\mu \otimes \gamma_\mu$  one-gluon-exchange interaction and  $1 \otimes 1$  linear confinement interaction between  $q$  and  $\bar{q}$ , which is given by

$$\tilde{V}^{\text{eff}} = \tilde{G}_{12} + \tilde{V}^{\text{cont}} + \tilde{V}^{\text{tens}} + \tilde{V}^{\text{so(v)}} + \tilde{S}_{12}(r) + \tilde{V}^{\text{so(s)}}, \quad (2.2)$$

where  $(\tilde{G}_{12})$ ,  $(\tilde{V}^{\text{cont}})$ ,  $(\tilde{V}^{\text{tens}})$ ,  $(\tilde{V}^{\text{so(v)})}$ ,  $[\tilde{S}_{12}(r)]$ , and  $(\tilde{V}^{\text{so(s)})}$ , are the Coulomb potential term, the contact potential term, the tensor potential term, the vector spin-orbit potential term, the screened confinement potential term and the scalar spin-orbit interaction term, respectively.

The spin-independent potential terms of the nonrelativistic potential read

$$\tilde{G}(r) = - \sum_k \frac{4\alpha_k}{3r} \left[ \frac{2}{\sqrt{\pi}} \int_0^{\gamma_k r} e^{-x^2} dx \right], \quad (2.3)$$

where  $\alpha_k = (0.25, 0.15, 0.2)$  and  $\gamma_k = (1/2, \sqrt{10}/2, \sqrt{1000}/2)$  for  $k = 1, 2, 3$  [16], and

$$S(r) = \frac{b(1 - e^{-\mu r})}{\mu} + c, \quad (2.4)$$

where  $\mu$  is the screened parameter given by our previous work [48].

The effective potential  $\tilde{V}^{\text{eff}}$  considered relativistic effects, particularly in meson systems, which are embedded in two ways. First, a smearing function for a meson  $q\bar{q}$  is introduced which has the form

$$\rho_{ij}(\mathbf{r} - \mathbf{r}') = \frac{\sigma_{ij}^3}{\pi^{3/2}} e^{-\sigma_{ij}^2(\mathbf{r}-\mathbf{r}')^2}, \quad (2.5)$$

with

$$\sigma_{ij}^2 = \sigma_0^2 \left[ \frac{1}{2} + \frac{1}{2} \left( \frac{4m_i m_j}{(m_i + m_j)^2} \right)^4 \right] + s^2 \left( \frac{2m_i m_j}{m_i + m_j} \right)^2, \quad (2.6)$$

where the values of  $\sigma_0$  and  $s$  are the parameters of the model. The Coulomb term  $\tilde{G}_{12}(r)$  is defined as

$$\tilde{G}_{ij}(r) = \int d^3\mathbf{r}' \rho_{ij}(\mathbf{r} - \mathbf{r}') G(r') = \sum_k -\frac{4\alpha_k}{3r} \text{erf}(\tau_{kij} r), \quad (2.7)$$

where the values of  $\tau_{kij}$  read

$$\tau_{kij} = \frac{1}{\sqrt{\frac{1}{\sigma_{ij}^2} + \frac{1}{\gamma_k^2}}}. \quad (2.8)$$

The potential  $\tilde{S}_{12}(r)$  can be expressed as

$$\begin{aligned} \tilde{S}_{12}(r) &= \int d^3\mathbf{r}' \rho_{12}(\mathbf{r} - \mathbf{r}') S(r') \\ &= \frac{b}{\mu r} \left[ r + e^{\frac{\mu^2}{4\sigma^2} + \mu r} \frac{\mu + 2r\sigma^2}{2\sigma^2} \left( \frac{1}{\sqrt{\pi}} \int_0^{\frac{\mu+2r\sigma^2}{2\sigma}} e^{-x^2} dx - \frac{1}{2} \right) \right. \\ &\quad \left. - e^{\frac{\mu^2}{4\sigma^2} - \mu r} \frac{\mu - 2r\sigma^2}{2\sigma^2} \left( \frac{1}{\sqrt{\pi}} \int_0^{\frac{\mu-2r\sigma^2}{2\sigma}} e^{-x^2} dx - \frac{1}{2} \right) \right] \\ &\quad + c. \end{aligned}$$

Second, due to relativistic effects, the general potential should depend on the mass of the interacting quarks. Momentum-dependent factors, which are unity in the nonrelativistic limit, are applied as

$$\tilde{G}_{12}(r) \rightarrow \tilde{G}_{12} = \left( 1 + \frac{\mathbf{p}^2}{E_1 E_2} \right)^{1/2} \tilde{G}_{12}(r) \left( 1 + \frac{\mathbf{p}^2}{E_1 E_2} \right)^{1/2}. \quad (2.9)$$

The semirelativistic correction of the spin-dependent terms are written as

$$\tilde{V}_{\alpha\beta}^i \rightarrow \tilde{V}_{\alpha\beta}^i = \left( \frac{m_\alpha m_\beta}{E_\alpha E_\beta} \right)^{1/2 + \epsilon_i} \tilde{V}_{\alpha\beta}^i \left( \frac{m_\alpha m_\beta}{E_\alpha E_\beta} \right)^{1/2 + \epsilon_i}, \quad (2.10)$$

where  $\tilde{V}_{\alpha\beta}^i(r)$  delegate the contact term, the tensor term, the vector term, and the scalar spin-orbit terms, and  $\epsilon_i = \epsilon_c, \epsilon_t, \epsilon_{\text{so(v)}},$  and  $\epsilon_{\text{so(s)}}$  impacts the potentials  $\tilde{V}^{\text{cont}}, \tilde{V}^{\text{tens}}, \tilde{V}^{\text{so(v)}},$  and  $\tilde{V}^{\text{so(s)}}$ , respectively [22]. They have the following forms

$$\tilde{V}^{\text{cont}} = \frac{2\mathbf{S}_1 \cdot \mathbf{S}_2}{3m_1 m_2} \nabla^2 \tilde{G}_{12}^c, \quad (2.11)$$

TABLE I: Parameters and their values in this work.

Parameter	value	Parameter	value
$m_u$ (GeV)	0.162	$\sigma_0$ (GeV)	1.791
$m_d$ (GeV)	0.162	$s$	0.711
$m_s$ (GeV)	0.377	$\mu$ (GeV)	0.0779
$b$ (GeV <sup>2</sup> )	0.222	$c$ (GeV)	-0.228
$\epsilon_c$	-0.137	$\epsilon_{so(v)}$	0.0550
$\epsilon_{so(s)}$	0.366	$\epsilon_t$	0.493

$$\widetilde{V}^{\text{tens}} = - \left( \frac{3\mathbf{S}_1 \cdot \mathbf{rS}_2 \cdot \mathbf{r}/r^2 - \mathbf{S}_1 \cdot \mathbf{S}_2}{3m_1m_2} \right) \left( \frac{\partial^2}{\partial r^2} - \frac{1}{r} \frac{1}{\partial r} \right) \widetilde{G}_{12}^t, \quad (2.12)$$

$$\begin{aligned} \widetilde{V}^{\text{so(v)}} = & \frac{\mathbf{S}_1 \cdot \mathbf{L}}{2m_1^2} \frac{1}{r} \frac{\partial \widetilde{G}_{11}^{\text{so(v)}}}{\partial r} + \frac{\mathbf{S}_2 \cdot \mathbf{L}}{2m_2^2} \frac{1}{r} \frac{\partial \widetilde{G}_{22}^{\text{so(v)}}}{\partial r} \\ & + \frac{(\mathbf{S}_1 + \mathbf{S}_2) \cdot \mathbf{L}}{m_1m_2} \frac{1}{r} \frac{\partial \widetilde{G}_{12}^{\text{so(v)}}}{\partial r}, \end{aligned} \quad (2.13)$$

$$\widetilde{V}^{\text{so(s)}} = - \frac{\mathbf{S}_1 \cdot \mathbf{L}}{2m_1^2} \frac{1}{r} \frac{\partial \widetilde{S}_{11}^{\text{so(s)}}}{\partial r} - \frac{\mathbf{S}_2 \cdot \mathbf{L}}{2m_2^2} \frac{1}{r} \frac{\partial \widetilde{S}_{22}^{\text{so(s)}}}{\partial r}. \quad (2.14)$$

After diagonalizing the Hamiltonian matrix as depicted in Eq. (2.1) under a simple harmonic oscillator (SHO) base, the mass and the spatial wave function of the meson can be obtained and applied to the strong decay process.

### B. The $^3P_0$ model

The  $^3P_0$  model (or QPC model) was initially raised by Micu [25] and further developed by the Orsay group [49–53]. This model is widely applied to calculate the OZI-allowed two-body strong decays of mesons [4, 6, 20–24, 26–46]. The  $\mathcal{T}$  operator describes a quark-antiquark pair (denoted by indices 3 and 4) creation from vacuum which reads  $J^{PC} = 0^{++}$ . For the process  $A \rightarrow B + C$ ,  $\mathcal{T}$  can be written as

$$\begin{aligned} \mathcal{T} = & -3\gamma \sum_m \langle 1m; 1 - m | 00 \rangle \int d\mathbf{p}_3 d\mathbf{p}_4 \delta^3(\mathbf{p}_3 + \mathbf{p}_4) \\ & \times \mathcal{Y}_{1m}^m \left( \frac{\mathbf{p}_3 - \mathbf{p}_4}{2} \right) \chi_{1,-m}^{34} \phi_0^{34} (\omega_0^{34})_{ij} b_{3i}^\dagger(\mathbf{p}_3) d_{4j}^\dagger(\mathbf{p}_4), \end{aligned} \quad (2.15)$$

where  $\mathcal{Y}_l^m(\vec{p}) \equiv p^l Y_l^m(\theta_p, \phi_p)$  is the solid harmonics.  $\chi$ ,  $\phi$ , and  $\omega$  denote the spin, flavor, and color wave functions respectively. Subindices  $i$  and  $j$  are the color index of the  $q\bar{q}$  pair. The amplitude  $M^{M_{J_A} M_{J_B} M_{J_C}}$  has the form

$$\langle BC | \mathcal{T} | A \rangle = \delta^3(\mathbf{P}_B + \mathbf{P}_C) \mathcal{M}^{M_{J_A} M_{J_B} M_{J_C}}. \quad (2.16)$$

Finally, the general form of the decay width can be expressed as

$$\Gamma = \frac{\pi}{4} \frac{|\mathbf{P}|}{m_A^2} \sum_{J,L} |\mathcal{M}^{JL}(\mathbf{P})|^2, \quad (2.17)$$

where  $m_A$  is the mass of the initial state  $A$ , and  $\mathbf{P}$  is the three-momentum of meson  $B$  in the rest frame of meson  $A$ . The two decay amplitudes can be related by the Jacob-Wick formula [54]

$$\begin{aligned} \mathcal{M}^{JL}(\mathbf{P}) = & \frac{\sqrt{4\pi(2L+1)}}{2J_A+1} \sum_{M_{J_B} M_{J_C}} \langle L0; JM_{J_A} | J_A M_{J_A} \rangle \\ & \times \langle J_B M_{J_B}; J_C M_{J_C} | J_A M_{J_A} \rangle \mathcal{M}^{M_{J_A} M_{J_B} M_{J_C}}. \end{aligned} \quad (2.18)$$

The parameter  $\gamma$  in this model depicts the strength of the creation of  $q\bar{q}$  from vacuum. In this work, we take the  $\gamma$  value to be 10.16 [48]. In our calculation, the spatial wave functions of mesons are obtained through the MGI model.

In the final states, the particles  $b_1$ ,  $h_1$ ,  $a_1$ ,  $a_2$ ,  $f_1$ ,  $f_2$ ,  $K_1$ , and  $K_1'$  correspond to the resonances  $b_1(1235)$ ,  $h_1(1170)$ ,  $a_1(1260)$ ,  $a_2(1320)$ ,  $f_1(1285)$ ,  $f_2(1270)$ ,  $K_1(1270)$ , and  $K_1(1400)$ , respectively. Other decay modes, such as  $\omega(2D)$ ,  $\omega(3D)$ ,  $K^*(3S)$ ,  $\phi(1D)$ ,  $\rho(4S)$ , and so on, represent the states that exist theoretically but have not yet been observed experimentally in Table V, and their mass is taken from the MGI model. Some decay channels with BR less than 1 are omitted.

## III. MASS SPECTRA AND TWO BODY STRONG DECAY OF THE HIGHLY EXCITED STATES OF $K_0^*$ FAMILY

In this section, we discuss the mass spectra and two body strong decay information of the highly excited states of  $0^+$  strange meson family. We start with the mass spectra.

### A. Mass spectra analysis

We employ the MGI model to calculate the mass spectra of  $0^+$  light strange meson family. The numerical result is demonstrated in Table II. The theoretical results and experimental values are shown in Table II.

For the  $1^3P_0$  state, our theoretical value (1284.3 MeV) remains  $\sim 140$  MeV below experimental value ( $1425 \pm 50$ ) MeV. GI model [55] predicts 1233 MeV ( $\sim 192$  MeV deficit), Ebert's result of 1362 MeV is still  $\sim 60$  MeV below experimental value. We will now focus on discussing the spectra of the highly excited states. Our predictions of  $3^3P_0$  (2184.8 MeV) overlap with experimental error bars of  $K_0^*(2130)$  ( $2128 \pm 40$  MeV), GI model shows  $\sim 230$  MeV deviation, and Ebert's result of 2160 MeV is also consistent with the experimental value. This result shows that introducing the color screening effect into the GI model can significantly improve the predictive power for the high-excited-state meson spectrum.

For  $K_0^*(4P)$  state, our theoretical mass of 2451 MeV is 300 MeV lower than the value given by the GI model. We predict

TABLE II: The mass spectra of  $n^3P_0$  states. The unit is MeV.

$n^{2s+1}L_J$	State	This work	GI [55]	Ebert [56]	Exp. [1]
$1^3P_0$	$K_0^*(1430)$	1284.3	1233	1362	$1425 \pm 50$ [1]
$2^3P_0$	$K_0^*(1950)$	1829.3	1890	1791	$1957 \pm 14$ [1]
$3^3P_0$	$K_0^*(2130)$	2184.8	2356	2160	$2128 \pm 31 \pm 9$ [57]
$4^3P_0$	$K_0^*(4P)$	2451.2	2749	–	–
$5^3P_0$	$K_0^*(5P)$	2658.9	3092	–	$2662 \pm 59 \pm 201$ [2]
$6^3P_0$	$K_0^*(6P)$	2831.8	3404	–	–

that  $K_0^*(5P)$  has the mass of 2658 MeV, which is in excellent agreement with the experimental central value.

We also calculate the mass of  $K_0^*(6P)$ , its value is 2832 MeV, approaching the mass range of charmed mesons.

Through the analysis of the mass spectrum, we conclude that the newly observed  $\kappa(2600)$  meson in experiments is a good candidate for the  $K_0^*(5P)$  state. Subsequently, we will further validate this conclusion by investigating its decay width and predicting the two-body strong decay properties of  $K_0^*(4P)$  and  $K_0^*(6P)$ .

### B. Strong decay analysis

In this section, we will discuss the two-body strong decay of the highly excited states of  $K_0^*$  family. At first, we will test our model with the ground state  $K_0^*$ . We obtain two decay channels of  $K_0^*(1430)$ ,  $K\pi$  and  $\eta K$  as shown in Table III.

The  $K\pi$  channel accounts for 95.5% of total width ( $\Gamma_{K\pi} = 252$  MeV), consistent with experimental branching ratio  $0.93 \pm 0.1$ . The predicted  $\Gamma_{\eta K} = 11.1$  MeV ( $\frac{\Gamma_{\eta K}}{\Gamma_{Total}} = 4.2\%$ ), which is slightly lower than the experimental value  $0.086_{-0.034}^{+0.037}$ . The calculated total width  $\Gamma_{total} = 264$  MeV shows excellent agreement with experimental data  $270 \pm 80$  MeV. These results show that the QPC model can work well for  $K_0^*(1430)$ , and we expect it to also be suitable for the highly excited states of  $K_0^*$  family.

TABLE III: The decay information of  $K_0^*(1430)$ . The unit of the width is MeV.

channel	width	BR	Exp [1].
$K\pi$	252	0.955	$0.93 \pm 0.1$
$\eta K$	11.1	0.042	$0.086_{-0.034}^{+0.037}$
Total width	264		$270 \pm 80$

The table provides the two-body strong decay information for the excited kaonic states:  $K_0^*(4P)$ ,  $\kappa(2600)(5P)$ , and  $K_0^*(6P)$ . These decays are crucial to understanding the resonance structures.

The dominant decay channel of  $K_0^*(4P)$  is  $K_1\pi$ , with a width

of 49.4 MeV, contributing 10.4% to the total width, which is much larger than the one obtained by Ref. [13]. Other significant decay modes include  $\pi K(4S)$  and  $K\pi$ , which contribute 8.15% and 6.11%, respectively.  $K\pi$  will be an ideal final channel to search the  $K_0^*(4P)$  state.  $K^*(1410)\rho$  and  $\pi K_1(2P)$  also have larger contributions to the total width about 5.7%.  $K^*(1410)\rho$  has the width of 32.5 MeV in Ref. [13]. The other decay channels with branching ratios less than 5% can be found in Table V. In the QPC model, the processes  $K_0^*(4P) \rightarrow K_0^*(1410)\omega$  and  $K_0^*(4P) \rightarrow K_0^*(1410)\rho$  share the same initial state  $K_0^*(4P)$  and the final state  $K^*(1410)$ . The wave functions of  $\omega$  and  $\rho$  are the same except the flavor wave functions. Combining the relationship  $m_\omega \simeq m_\rho$ , their decay outcomes depend on the overlap of the flavor matrix elements. Finally, we can roughly obtain  $\frac{\Gamma_{K^*(1410)\rho}}{\Gamma_{K^*(1410)\omega}} \simeq 3$ . In our calculation,  $\frac{\Gamma_{K^*(1410)\rho}}{\Gamma_{K^*(1410)\omega}} \simeq 3.31$ . Another relation,  $\frac{\Gamma_{K^*\rho}}{\Gamma_{K^*\omega}} \simeq 3.17$ , is also consistent with 3. The other decay channels can be found in Table V. The total width of  $K_0^*(4P)$  is 475 MeV, which is three times larger than that of Ref. [13].

For the  $\kappa(2600)(5P)$ , the largest decay channel is also  $K_1\pi$ , accounting for 7.5% of the total width.  $K^*(1410)\rho$  is comparably significant (6.39%). This state also exhibits considerable decay fractions into higher excitations, such as  $\pi K_1(2P)$  and  $Kb_1(1960)$ , which contribute larger than 4%. The  $K\pi$  channel constitutes a major decay mode of this  $\kappa(2600)(5P)$  state, consistent with its experimental observation in the same channel.  $\pi K_1(3P)$ ,  $\pi K(5S)$ ,  $\pi K_2(2D)$ ,  $Ka_1(1640)$ , and  $\pi K(4S)$ , all have a significant contribution to the total width of  $\kappa(2600)(5P)$ , with branch ratios being all about 3%. The other decay channels of  $\kappa(2600)(5P)$  with branching ratios less than 3% can be found in Table V. The important thing is the total decay width of  $\kappa(2600)(5P)$  overlaps with the experimental value  $480 \pm 47 \pm 72$  MeV. This result supports our classification of  $\kappa(2600)$  as the  $K_0^*(5P)$  resonance.

$K_0^*(6P)$  configuration demonstrates remarkable parallels to  $K_0^*(5P)$ , with the dominant eight decay channels showing negligible divergence. The most important decay modes include  $K^*(1410)\rho$  (5.7%) and  $K_1\pi$  (5.5%).  $\pi K_1(2P)$ ,  $Kb_1(1960)$ ,  $\pi K_1(3P)$ , and  $\pi K_2(2D)$  are its larger decay channels with branch ratios of 3.1% to 3.8%. As in  $K_0^*(5P)$ , the  $K\pi$  channel constitutes a major decay mode of this  $K_0^*(6P)$  state. Ex-

TABLE IV: The two body strong decay information of  $K_0^*(4P)$  state,  $\kappa(2600)(5P)$  state, and  $K_0^*(6P)$  state. The unit of the width is MeV.

$K_0^*(4P)$				$\kappa(2600)(5P)$			$K_0^*(6P)$		
channel	width	BR	Wang [13]	channel	width	BR	channel	width	BR
$K_1\pi$	49.4	0.104	0.02	$K_1\pi$	32.4	0.0751	$K^*(1410)\rho$	21.6	0.0568
$\pi K(4S)$	38.7	0.0815	–	$K^*(1410)\rho$	27.6	0.0639	$K_1\pi$	20.8	0.0548
$K\pi$	29.1	0.0611	0.6	$\pi K_1(2P)$	20.1	0.0466	$\pi K_1(2P)$	14.6	0.0384
$K^*(1410)\rho$	27.3	0.0575	32.5	$Kb_1(1960)$	18.5	0.0428	$Kb_1(1960)$	13.7	0.036
$\pi K_1(2P)$	27.1	0.057	–	$K\pi$	17.1	0.0395	$\pi K_1(3P)$	11.8	0.0312
$K\pi(1300)$	20.8	0.0438	0.16	$\pi K_1(3P)$	14.7	0.0341	$\pi K_2(2D)$	11.6	0.0305
$\pi K(3S)$	19.3	0.0406	–	$\pi K(5S)$	14.5	0.0335	$K\pi$	10.8	0.0283
$Ka_1(1640)$	19.1	0.0402	0.23	$\pi K_2(2D)$	14.1	0.0327	$\pi K(5S)$	9.69	0.0255
$\pi K(1460)$	17.4	0.0367	0.12	$Ka_1(1640)$	13.7	0.0318	$Ka_3(2030)$	9.68	0.0255
$K^*\rho$	16	0.0338	8.76	$K\pi(1300)$	13.1	0.0304	$\pi K'_1(5P)$	8.95	0.0236
$Ka_1$	14.5	0.0304	0.7	$\pi K(4S)$	13.1	0.0302	$K\pi(1300)$	8.87	0.0233
$\pi K_2(2D)$	13.6	0.0286	–	$\pi K(1460)$	11.5	0.0265	$\pi K_2(4D)$	8.63	0.0227
$\pi K_1(3P)$	13.3	0.0281	–	$\pi K'_1(4P)$	11	0.0254	$\pi K(1460)$	8.16	0.0215
$K\pi_2(1880)$	13.2	0.0277	7.15	$K^*a_1(1640)$	10.9	0.0254	$Ka_1(1640)$	8.13	0.0214
$\pi K'_1(3P)$	11.4	0.0239	–	$\pi K(3S)$	9.85	0.0228	$\pi K_1(4P)$	7.63	0.0201
$Kb_1(2P)$	10.3	0.0217	–	$K\pi_2(1880)$	9.84	0.0228	$\pi K(4S)$	7.39	0.0194
$h_1(1595)K$	10.3	0.0216	4.6	$\omega K^*(1410)$	8.66	0.0201	$K\pi(1800)$	7.31	0.0193
$K^*\rho(1450)$	9.55	0.0201	6.34	$K\pi(1800)$	8.46	0.0196	$K^*a_1(1640)$	7.29	0.0192
$K^*a_1$	9.18	0.0193	2.5	$Ka_1$	7.74	0.0179	$\pi K'_3(2F)$	7.25	0.0191
$K\pi(1800)$	8.77	0.0185	–	$\pi K_3(1F)$	7.24	0.0168	$\omega K^*(1410)$	6.87	0.0181
$Kb_1$	8.37	0.0176	4.5	$Kb_1(2P)$	6.89	0.016	$\pi K_3(1F)$	6.4	0.0169
$\omega K^*(1410)$	8.24	0.0173	36.8	$Ka_3(2030)$	6.77	0.0157	$K\pi_2(1880)$	6.2	0.0163
$\pi K_3(1F)$	6.02	0.0127	–	$h_1(1595)K$	6.31	0.0146	$\pi K(3S)$	5.89	0.0155
$K'_1\rho$	5.41	0.0114	< 0.01	$K^*\rho$	6.1	0.0141	$K_1b_1$	5.64	0.0148
$\omega K^*$	5.05	0.0106	8.15	$K_1b_1$	6.08	0.0141	$\pi K'_1(4P)$	5.3	0.0139
$K^*f_1$	4.91	0.0103	0.34	$K^*a_1$	5.25	0.0122	$K^*(1410)a_1$	4.76	0.0125
				$\pi K'_3(2F)$	4.89	0.0113	$Kb_1(2P)$	4.67	0.0123
				$K^*\rho(1450)$	4.44	0.0103	$h_1(1595)K$	4.32	0.0114
				$\pi K'_1(3P)$	4.35	0.0101	$Ka_1$	4.18	0.011
Total width	475		180	Total width	432		Total width	380	

periments can search for this state through the  $K\pi$  final channel. This state exhibits a more evenly distributed decay pattern, with multiple channels contributing between 2-4% each. Other decay channels of  $K_0^*(6P)$  with more details are listed in Table V. We find that the total width of  $K_0^*(6P)$  is 380 MeV.

#### IV. CONCLUSION

In this work, we have systematically studied the mass spectra and the OZI-allowed two-body strong decay behaviors of the newly observed  $\kappa(2600)$ , along with the higher excited kaonic states,  $K_0^*(4P)$  and  $K_0^*(6P)$ .

The newly observed state  $\kappa(2600)$  is a good candidate for the  $K_0^*(5P)$  state. The findings are supported not only by the Regge trajectory and the MGI model results, but also through an analysis of the QPC model. The total and branching decay

widths allow for the identification of  $\kappa(2600)$  as the  $K_0^*(5P)$  state. Its two most important decay channels are  $K_1\pi$  and  $K^*(1410)\rho$ .

The masses of  $K_0^*(4P)$  state and  $K_0^*(6P)$  states were predicted to be about 2450 MeV and 2830 MeV, respectively. The total widths for the  $K_0^*(4P)$  state and  $K_0^*(6P)$  state are about 475 MeV and 380 MeV, respectively. The  $K\pi$  channel is an ideal final channel for searching these two  $K_0^*$  states.  $K_1\pi$  and  $\pi K(4S)$  are two of the most important decay channels of the  $K_0^*(4P)$  state, with branch ratios of 10.4% and 8.2% respectively. The branch ratio of  $K\pi$  channel is about 6% for the  $K_0^*(4P)$  state. The  $K^*(1410)\rho$  and  $K_1\pi$  channels are two main final states of the  $K_0^*(6P)$  state, and they have branch ratios larger than 5%.

We look forward to future experimental studies, which will play a crucial role in searching for the higher excited states of kaons.

TABLE V: The two body strong decay information of  $K_0^*(4P)$  state,  $\kappa(2600)(5P)$  state, and  $K_0^*(6P)$  state. The unit of the width is MeV.

$K_0^*(4P)$			$\kappa(2600)(5P)$			$K_0^*(6P)$		
channel	width	BR	channel	width	BR	channel	width	BR
$K_1\pi$	49.4	0.104	$K_1\pi$	32.4	0.0751	$K^*(1410)\rho$	21.6	0.0568
$\pi K(4S)$	38.7	0.0815	$K^*(1410)\rho$	27.6	0.0639	$K_1\pi$	20.8	0.0548
$K\pi$	29.1	0.0611	$\pi K_1(2P)$	20.1	0.0466	$\pi K_1(2P)$	14.6	0.0384
$K^*(1410)\rho$	27.3	0.0575	$Kb_1(1960)$	18.5	0.0428	$Kb_1(1960)$	13.7	0.036
$\pi K_1(2P)$	27.1	0.057	$K\pi$	17.1	0.0395	$\pi K_1(3P)$	11.8	0.0312
$K\pi(1300)$	20.8	0.0438	$\pi K_1(3P)$	14.7	0.0341	$\pi K_2(2D)$	11.6	0.0305
$\pi K(3S)$	19.3	0.0406	$\pi K(5S)$	14.5	0.0335	$K\pi$	10.8	0.0283
$Ka_1(1640)$	19.1	0.0402	$\pi K_2(2D)$	14.1	0.0327	$\pi K(5S)$	9.69	0.0255
$\pi K(1460)$	17.4	0.0367	$Ka_1(1640)$	13.7	0.0318	$Ka_3(2030)$	9.68	0.0255
$K^*\rho$	16	0.0338	$K\pi(1300)$	13.1	0.0304	$\pi K'_1(5P)$	8.95	0.0236
$Ka_1$	14.5	0.0304	$\pi K(4S)$	13.1	0.0302	$K\pi(1300)$	8.87	0.0233
$\pi K_2(2D)$	13.6	0.0286	$\pi K(1460)$	11.5	0.0265	$\pi K_2(4D)$	8.63	0.0227
$\pi K_1(3P)$	13.3	0.0281	$\pi K'_1(4P)$	11	0.0254	$\pi K(1460)$	8.16	0.0215
$K\pi_2(1880)$	13.2	0.0277	$K^*a_1(1640)$	10.9	0.0254	$Ka_1(1640)$	8.13	0.0214
$\pi K'_1(3P)$	11.4	0.0239	$\pi K(3S)$	9.85	0.0228	$\pi K_1(4P)$	7.63	0.0201
$Kb_1(2P)$	10.3	0.0217	$K\pi_2(1880)$	9.84	0.0228	$\pi K(4S)$	7.39	0.0194
$h_1(1595)K$	10.3	0.0216	$\omega K^*(1410)$	8.66	0.0201	$K\pi(1800)$	7.31	0.0193
$K^*\rho(1450)$	9.55	0.0201	$K\pi(1800)$	8.46	0.0196	$K^*a_1(1640)$	7.29	0.0192
$K^*a_1$	9.18	0.0193	$Ka_1$	7.74	0.0179	$\pi K'_3(2F)$	7.25	0.0191
$K\pi(1800)$	8.77	0.0185	$\pi K_3(1F)$	7.24	0.0168	$\omega K^*(1410)$	6.87	0.0181
$Kb_1$	8.37	0.0176	$Kb_1(2P)$	6.89	0.016	$\pi K_3(1F)$	6.4	0.0169
$\omega K^*(1410)$	8.24	0.0173	$Ka_3(2030)$	6.77	0.0157	$K\pi_2(1880)$	6.2	0.0163
$\pi K_3(1F)$	6.02	0.0127	$h_1(1595)K$	6.31	0.0146	$\pi K(3S)$	5.89	0.0155
$K'_1\rho$	5.41	0.0114	$K^*\rho$	6.1	0.0141	$K_1b_1$	5.64	0.0148
$\omega K^*$	5.05	0.0106	$K_1b_1$	6.08	0.0141	$\pi K'_1(4P)$	5.3	0.0139
$K^*f_1$	4.91	0.0103	$K^*a_1$	5.25	0.0122	$K^*(1410)a_1$	4.76	0.0125
			$\pi K'_3(2F)$	4.89	0.0113	$Kb_1(2P)$	4.67	0.0123
			$K^*\rho(1450)$	4.44	0.0103	$h_1(1595)K$	4.32	0.0114
			$\pi K'_1(3P)$	4.35	0.0101	$Ka_1$	4.18	0.011
Total width	475		Total width	432		Total width	380	

### Acknowledgments

This work is supported by the National Natural Science Foundation of China under Grants No. 11965016, and

No. 12247101, and by the Natural Science Foundation of Qinghai Province under Grant No. 2022-ZJ-939Q, the Fundamental Research Funds for the Central Universities (Grant No. lzujbky-2024-jdzx06).

- 
- [1] S. Navas *et al.* (Particle Data Group), *Phys. Rev. D* **110**, 030001 (2024).
- [2] R. Aaij *et al.* (LHCb), *Phys. Rev. D* **108**, 032010 (2023), [arXiv:2304.14891 \[hep-ex\]](#).
- [3] T.-G. Li, S.-C. Zhang, G.-Y. Wang, and Q.-F. Lü, *Phys. Rev. D* **110**, 114020 (2024), [arXiv:2404.17246 \[hep-ph\]](#).
- [4] T.-Y. Li, Y.-R. Wang, and C.-Q. Pang, *Phys. Rev. D* **107**, 074008 (2023), [arXiv:2205.02157 \[hep-ph\]](#).
- [5] T. Barnes, N. Black, and P. R. Page, *Phys. Rev. D* **68**, 054014 (2003), [arXiv:nucl-th/0208072 \[nucl-th\]](#).
- [6] C.-Q. Pang, J.-Z. Wang, X. Liu, and T. Matsuki, *Eur. Phys. J. C* **77**, 861 (2017), [arXiv:1705.03144 \[hep-ph\]](#).
- [7] R. L. Jaffe, *Phys. Rept.* **409**, 1 (2005), [arXiv:hep-ph/0409065](#).
- [8] G. 't Hooft, G. Isidori, L. Maiani, A. D. Polosa, and V. Riquer, *Phys. Lett. B* **662**, 424 (2008), [arXiv:0801.2288 \[hep-ph\]](#).
- [9] F. E. Close and N. A. Tornqvist, *J. Phys. G* **28**, R249 (2002), [arXiv:hep-ph/0204205](#).
- [10] D. Parganlija, P. Kovacs, G. Wolf, F. Giacosa, and

- D. H. Rischke, *AIP Conf. Proc.* **1520**, 226 (2013), [arXiv:1208.5611 \[hep-ph\]](#) .
- [11] J. R. Pelaez, *Phys. Rev. Lett.* **92**, 102001 (2004), [arXiv:hep-ph/0309292](#) .
- [12] G. Eichmann, C. S. Fischer, and W. Heupel, *Phys. Lett. B* **753**, 282 (2016), [arXiv:1508.07178 \[hep-ph\]](#) .
- [13] T.-G. Li, Z. Gao, G.-Y. Wang, D.-M. Li, E. Wang, and J. Zhu, *Phys. Rev. D* **106**, 034012 (2022), [arXiv:2203.17082 \[hep-ph\]](#) .
- [14] G. F. Chew and S. C. Frautschi, *Phys. Rev. Lett.* **8**, 41 (1962).
- [15] A. Anisovich, V. Anisovich, and A. Sarantsev, *Phys. Rev. D* **62**, 051502 (2000), [arXiv:hep-ph/0003113 \[hep-ph\]](#) .
- [16] S. Godfrey and N. Isgur, *Phys. Rev. D* **32**, 189 (1985).
- [17] E. van Beveren and G. Rupp, *Phys. Rev. Lett.* **91**, 012003 (2003), [arXiv:hep-ph/0305035 \[hep-ph\]](#) .
- [18] Y.-R. Liu, X. Liu, and S.-L. Zhu, *Phys. Rev. D* **79**, 094026 (2009), [arXiv:0904.1770 \[hep-ph\]](#) .
- [19] Y. B. Dai, X. Q. Li, S. L. Zhu, and Y. B. Zuo, *European Physical Journal C* **55**, 249 (2008).
- [20] C.-Q. Pang, Y.-R. Wang, and C.-H. Wang, *Phys. Rev. D* **99**, 014022 (2019), [arXiv:1810.02694 \[hep-ph\]](#) .
- [21] Y.-R. Wang, T.-Y. Li, Z.-Y. Fang, H. Chen, and C.-Q. Pang, *Phys. Rev. D* **106**, 114024 (2022), [arXiv:2208.10329 \[hep-ph\]](#) .
- [22] L.-M. Wang, S.-Q. Luo, and X. Liu, *Phys. Rev. D* **105**, 034011 (2022), [arXiv:2109.06617 \[hep-ph\]](#) .
- [23] L.-M. Wang, W.-X. Tian, and X. Liu, (2024), [arXiv:2408.05908 \[hep-ph\]](#) .
- [24] X.-C. Feng, Z.-Y. Li, D.-M. Li, Q.-T. Song, E. Wang, and W.-C. Yan, *Phys. Rev. D* **106**, 076012 (2022), [arXiv:2206.10132 \[hep-ph\]](#) .
- [25] L. Micu, *Nucl. Phys. B* **10**, 521 (1969).
- [26] E. van Beveren, G. Rupp, T. Rijken, and C. Dullemond, *Phys. Rev. D* **27**, 1527 (1983).
- [27] A. I. Titov, T. I. Gulamov, and B. Kampfer, *Phys. Rev. D* **53**, 3770 (1996).
- [28] E. Ackleh, T. Barnes, and E. Swanson, *Phys. Rev. D* **54**, 6811 (1996), [arXiv:hep-ph/9604355 \[hep-ph\]](#) .
- [29] H. G. Blundell, [hep-ph/9608473](#) (1996).
- [30] R. Bonnaz, B. Silvestre-Brac, and C. Gignoux, *Eur. Phys. J. A* **13**, 363 (2002), [arXiv:hep-ph/0101112 \[hep-ph\]](#) .
- [31] H. Q. Zhou, R. G. Ping, and B. S. Zou, *Phys. Lett. B* **611**, 123 (2005), [arXiv:hep-ph/0412221 \[hep-ph\]](#) .
- [32] J. Lu, X.-L. Chen, W.-Z. Deng, and S.-L. Zhu, *Phys. Rev. D* **73**, 054012 (2006), [arXiv:hep-ph/0602167 \[hep-ph\]](#) .
- [33] B. Zhang, X. Liu, W.-Z. Deng, and S.-L. Zhu, *Eur. Phys. J. C* **50**, 617 (2007), [arXiv:hep-ph/0609013 \[hep-ph\]](#) .
- [34] Z.-G. Luo, X.-L. Chen, and X. Liu, *Phys. Rev. D* **79**, 074020 (2009), [arXiv:0901.0505 \[hep-ph\]](#) .
- [35] Z.-F. Sun and X. Liu, *Phys. Rev. D* **80**, 074037 (2009), [arXiv:0909.1658 \[hep-ph\]](#) .
- [36] X. Liu, Z.-G. Luo, and Z.-F. Sun, *Phys. Rev. Lett.* **104**, 122001 (2010), [arXiv:0911.3694 \[hep-ph\]](#) .
- [37] Z.-F. Sun, J.-S. Yu, X. Liu, and T. Matsuki, *Phys. Rev. D* **82**, 111501 (2010), [arXiv:1008.3120 \[hep-ph\]](#) .
- [38] T. Rijken, M. Nagels, and Y. Yamamoto, *Nucl. Phys. A* **835**, 160 (2010).
- [39] Z.-C. Ye, X. Wang, X. Liu, and Q. Zhao, *Phys. Rev. D* **86**, 054025 (2012), [arXiv:1206.0097 \[hep-ph\]](#) .
- [40] X. Wang, Z.-F. Sun, D.-Y. Chen, X. Liu, and T. Matsuki, *Phys. Rev. D* **85**, 074024 (2012), [arXiv:1202.4139 \[hep-ph\]](#) .
- [41] L.-P. He, X. Wang, and X. Liu, *Phys. Rev. D* **88**, 034008 (2013), [arXiv:1306.5562 \[hep-ph\]](#) .
- [42] Y. Sun, X. Liu, and T. Matsuki, *Phys. Rev. D* **88**, 094020 (2013), [arXiv:1309.2203 \[hep-ph\]](#) .
- [43] Y.-R. Wang, Y. Ma, and C.-Q. Pang, *Int. J. Mod. Phys. A* **38**, 2350118 (2023), [arXiv:2211.09023 \[hep-ph\]](#) .
- [44] T.-Y. Li, L. Tang, Z.-Y. Fang, C.-H. Wang, C.-Q. Pang, and X. Liu, *Phys. Rev. D* **108**, 034019 (2023), [arXiv:2204.14258 \[hep-ph\]](#) .
- [45] L.-M. Wang, Q.-S. Zhou, C.-Q. Pang, and X. Liu, *Phys. Rev. D* **102**, 114034 (2020), [arXiv:2010.05132 \[hep-ph\]](#) .
- [46] J.-C. Feng, X.-W. Kang, Q.-F. Lü, and F.-S. Zhang, *Phys. Rev. D* **104**, 054027 (2021), [arXiv:2104.01339 \[hep-ph\]](#) .
- [47] Q.-T. Song, D.-Y. Chen, X. Liu, and T. Matsuki, *Phys. Rev. D* **91**, 054031 (2015), [arXiv:1501.03575 \[hep-ph\]](#) .
- [48] Y.-R. Wang, X.-H. Liu, C.-Q. Pang, and H. Chen, *Phys. Rev. D* **111**, 054005 (2025).
- [49] A. Le Yaouanc, L. Oliver, O. Pene, and J. Raynal, *Phys. Rev. D* **8**, 2223 (1973).
- [50] A. Le Yaouanc, L. Oliver, O. Pene, and J.-C. Raynal, *Phys. Rev. D* **9**, 1415 (1974).
- [51] A. Le Yaouanc, L. Oliver, O. Pene, and J. Raynal, *Phys. Rev. D* **11**, 1272 (1975).
- [52] A. Le Yaouanc, L. Oliver, O. Pene, and J. Raynal, *Phys. Lett. B* **72**, 57 (1977).
- [53] A. Le Yaouanc, L. Oliver, O. Pene, and J.-C. Raynal, *Phys. Lett. B* **71**, 397 (1977).
- [54] M. Jacob and G. Wick, *Annals Phys.* **7**, 404 (1959).
- [55] S. Godfrey, *AIP Conf. Proc.* **132**, 262 (1985).
- [56] D. Ebert, R. Faustov, and V. Galkin, *Phys. Rev. D* **79**, 114029 (2009), [arXiv:0903.5183 \[hep-ph\]](#) .
- [57] J. P. Lees et al. (BaBar), *Phys. Rev. D* **104**, 072002 (2021), [arXiv:2106.05157 \[hep-ex\]](#) .